Cement and Concrete Research 38 (2008) 1261–1269

Contents lists available at ScienceDirect

Cement and Concrete Research

journal homepage: http://ees.elsevier.com/CEMCON/default.asp

Crystal structure of low magnesium-content alite: Application to Rietveld quantitative phase analysis

Ángeles G. De la Torre, Ruth N. De Vera, Antonio J.M. Cuberos, Miguel. A.G. Aranda *

Departamento de Química Inorgánica, Cristalografía y Mineralogía. Universidad de Málaga. Campus de Teatinos. 29071-Málaga, Spain

A R T I C L E I N F O

Article history:
Received 19 February 2008
Accepted 26 June 2008

A B S T R A C T

Five members of tricalcium silicate solid solution, $Ca_{3-x-y}Mg_xAl_y(Si_{1-y}Al_y)O_5$, have been prepared. T_1, T_3 and M_3 forms have been identified by X-ray powder diffraction, but pure M_1 form was not stabilized. The crystal structure of a sample nominally $Ca_{2.96}Mg_{0.03}Al_{0.01}(Si_{0.99}Al_{0.01})O_5$ has been studied by a joint Rietveld refinement using strictly monochromatic laboratory X-ray and neutron powder diffraction data, with soft constraints of interatomic distances. The crystal structure of this alite is a T_3 form with a triclinic cell, space group $P\bar{1}$, of dimensions $a=11.6389(2)$ Å, $b=14.1716(3)$ Å, $c=13.6434(3)$ Å, $\alpha=104.982(2)°$, $\beta=94.622(1)°$, $\gamma=90.107(2)°$ and $V/Z=120.346(6)$ Å^3. Laboratory and commercial clinkers were studied by synchrotron X-ray powder diffraction and the Rietveld method. The reported T_3 structure for alite fits properly a variety of laboratory Portland clinkers with low magnesium contents. The alite refined volume(s) (V/Z) is useful to predict the magnesium oxide content of a clinker and the alite-type. Thus, a refined V/Z value between 121.0 and 120.3 Å^3 should contain up to ~1.0 wt.% of MgO, being T_3 type. If refined C_3S V/Z is smaller than ~119.8 Å^3 the clinker may contain more than ~2.1 wt.% of MgO with alite as M_3. For intermediate magnesium (and sulfur) contents, alites phase coexistence may be detected by using strictly monochromatic laboratory or synchrotron X-ray powder diffraction. However, the application of these results to commercial materials has to be taken cautiously due to the influence of other foreign ions in volume and alite-type.

1. Introduction

During this decade, there has been great deal of interest in the quantitative phase analysis (QPA) of complex mixtures [1,2] such as anhydrous cements [3–6] or hydrated systems [7,8] from X-ray powder diffraction data using Rietveld methodology. To do so, the crystal structures of all components in the mixtures must be known. Therefore, the crystal structure of the main component of Portland cements, i.e. tricalcium silicate [Ca_3SiO_5 or C_3S], should be well known, if accurate Rietveld QPA is to be performed. The room-temperature (RT) polymorph of stoichiometric C_3S presents a triclinic structure [9]. Stoichiometric Ca_3SiO_5 exhibits seven polymorphs on heating: three triclinics (T_1, T_2, T_3), three monoclinics (M_1, M_2, M_3) and one rhombohedral (R). The phase transformations are $T_1 \leftrightarrows T_2 \leftrightarrows T_3 \leftrightarrows M_1 \leftrightarrows M_2 \leftrightarrows M_3 \leftrightarrows R$ at 620, 920, 980, 990, 1060 and 1070 °C, respectively [10,11]. However, the presence of foreign ions may stabilise some of the high-temperature forms at RT. For instance, Mg and/or sulphate ions stabilise the M_1 and/or M_3 monoclinic forms [12]. These non-stoichiometric phases are commonly named alites. However, all these structures are very complex, i.e. most of them present superstructures (modulated structures), and they are not fully understood [13,14]. For instance, Peterson [15] concluded that a powder pattern of unmodulated T_3 form can be justified by using a structural description derived from T_1 [9]. Atomic parameters for an average T_3-structure were reported from synchrotron powder diffraction data [16].

On the other hand, an average M_1 structural description was published and tested in the Rietveld quantitative phase analysis of industrial clinkers [17]. The structural models available to describe the different polymorphs, T_1 [9] and R [18], or M-alites [17,19,20] differ by the silicate tetrahedral orientations.

The main objective of this work is to obtain a crystal structure for low magnesium-bearing alite, in order to carry out Rietveld quantitative phase analyses of industrial clinkers. C_3S presents a complex structure, so it is advisable to perform a structural study using both laboratory X-ray and neutron powder diffraction data. The latter is a complementary structural technique since it allows to accurately locate the light atoms such as oxygens. The second objective is to test the new structural description for the mineralogical analysis of clinkers with variable Mg-content.

2. Experimental section

2.1. Samples preparation

2.1.1. Tricalcium silicate solid solution

A five-member series of tricalcium silicate solid solution has been prepared with nominal stoichiometry: $Ca_{3-x-y}Mg_xAl_y(Si_{1-y}Al_y)O_5$, x

---

* Corresponding author.
E-mail address: g_aranda@uma.es (M.A.G. Aranda).

0008-8846/$ – see front matter © 2008 Elsevier Ltd. All rights reserved.
doi:10.1016/j.cemconres.2008.06.005

Table 1
Molar magnesium and aluminum contents for $Ca_{3-x-y}Mg_xAl_y(Si_{1-y}Al_y)O_5$ (nominal stoichiometries)

Sample	x	y	TT
C_3S–00 Mg00Al	0.0	0.0	2
C_3S–03 Mg01Al	0.03	0.01	1
C_3S–03 Mg02Al	0.03	0.02	2
C_3S–06 Mg01Al	0.06	0.01	2
C_3S–06 Mg02Al	0.06	0.02	1

TT stands for the number of thermal treatments up to 1500 °C during 6 h.

and y values are given in Table 1. These compounds were synthesized by conventional ceramic method using high purity oxides and carbonates as starting materials: SiO_2 (ABCR, quartz powder 99.6% with 0.2 wt.% being volatile impurities), $CaCO_3$ (Alfa, 99.95%), $Mg(OH)_2\cdot 4MgCO_3\cdot 5H_2O$ (99% from Aldrich) and γ-Al_2O_3 (Alfa, 99.997%). Raw materials were ground for 30 min in a Fritsch planetary ball mill (model Pulverisette 7, 45 cm^3 agate vessel containing 7 agate balls with a diameter of 15 mm) at 200 rpm with reverse rotation each 10 min and heated at 1000 °C for 6 h. The resulting powders were reground in the planetary ball mill, pelletized and heated in air at 1500 °C for 6 h. These final mechanical and thermal treatments were repeated until no free lime (CaO) was observed in the X-ray powder diffraction patterns. Final samples were ground to a fine powder before collecting X-ray powder diffraction data.

2.1.2. Laboratory ordinary Portland clinkers

The elemental composition of calcite, shown in Table 2, was determined by X-ray fluorescence spectroscopy on Phillips PW-1404 spectrophotometer. The elemental composition of kaolin, Table 2, was measured by inductively coupled plasma atomic emission spectroscopy (ICP-AES) on an IRIS Advantage instrument from Thermo Jarrel Ash.

Ordinary Portland clinkers were prepared by mixing ~75 wt.% of calcite (99% Aldrich), ~10 wt.% of kaolin (Aldrich), ~11 wt.% of quartz (99.6% ABCR) and ~4 wt.% of iron oxide (99.95% AlfaAesar). Appropriated amounts of MgO and SO_3 were also added as $Mg(OH)_2\cdot 4MgCO_3\cdot 5H_2O$ (99% from Aldrich) and $CaSO_4\cdot 2H_2O$ (ground gypsum single crystals, this powder being single phase by X-ray powder diffraction), respectively; in order to study the influence of these elements in the mineralogical composition. Table 2 gives the nominal dosages, expressed as oxide, used to prepare all the clinkers, obtained from elemental composition of raw materials. One series (5 clinkers) was prepared with increasing amounts MgO and a fixed value of SO_3, i.e. ~0.75 wt.%. The remaining clinkers contain 1.20 wt.% of SO_3, Cl–1.5 Mg-b and Cl–2.5 Mg-b. Raw materials were mixed in an agate mortar with the aid of ethanol and dried in a stove at 60 °C. This treatment was performed three times. The clinkerization was carried out by pressing the raw mixtures into pellets of 16 mm of diameter. The pellets were placed on Pt/Rh crucibles and heated at 5 °C/min to 900 °C, which was held for 30 min. The temperature was then raised at a rate of 5 °C/min up to 1450 °C and held for 15 min. Finally, the clinkers were cooled from the highest temperature applying air flow (approximate cooling rate of 2000 °C/min). These clinkers were ground to a fine powder before collecting X-ray powder diffraction data.

Table 2 also includes elemental composition obtained by X-ray fluorescence of two commercial materials, a white Portland clinker: CC_W and a grey Portland clinker: CC_G.

2.2. X-ray data collection

All members of the C_3S solid solution were characterized by laboratory X-ray powder diffraction (LXRPD) at room temperature. The powder patterns were collected on a PANalytical X'Pert Pro MPD automated diffractometer equipped with a Ge(111) primary monochromator (strictly monochromatic $CuK\alpha_1$ radiation) and an X'Celerator detector. The overall measurement time was ~4 h per pattern to have good statistics over the 10.0 to 70.0° (2Θ) angular range, with 0.017° step size.

Synchrotron X-ray powder diffraction (SXRPD) patterns of laboratory and commercial Portland clinkers were collected on ID31 diffractometer of European Synchrotron Radiation Facility, (ESRF, Grenoble, France) in Debye-Scherrer (transmission) configuration. The samples were loaded in borosilicate glass capillaries (d=1.5 mm) and rotated during data collection. In each experiment, the wavelength was selected with a double-crystal Si (111) monochromator and calibrated with Si NIST SRM 640b (a=5.43094 Å). The measurement range was 2.5 to 30° (2Θ) and the data were normalized and summed up to 0.003° step size. The wavelengths used for studying the clinkers are given in Table 2.

2.3. Neutron powder diffraction data collection

Neutron powder diffraction (NPD) data were also collected for nominal $Ca_{2.96}Mg_{0.03}Al_{0.01}(Si_{0.99}Al_{0.01})O_5$, [hereafter C_3S–03 Mg01Al], on HRPT diffractometer [21] of SINQ (Villigen, Switzerland) using a wavelength of 1.1886 Å. This pattern had very good statistics (overall counting time ~5 h) and the data range was 10.0 to 160.0° (2Θ) with a step size of 0.05°.

2.4. Rietveld analysis

All Rietveld [22] analyses were done using the GSAS suite of programs [23]. Final global optimized parameters were: background coefficients, cell parameters, zero-shift error, peak shape parameters

Table 2
Chemical composition of raw materials: calcite and kaolin

	CaO	SiO_2	Al_2O_3	Fe_2O_3	K_2O	Na_2O	MgO	SO_3	SrO	LOI*	λ
Calcite	55.91	0.01	–	–	–	0.09	0.01	0.01	0.08	43.89	
Kaolin	0.09	47.25	37.46	0.49	1.58	0.14	0.33			12.41	
Cl–0.4MgO	65.65	21.16	6.31	5.21	0.27	0.13	0.38	0.76	0.09	0.70	0.620706(2)
Cl–1.1MgO	64.69	21.3	6.36	5.24	0.27	0.13	1.13	0.76	0.09	1.08	0.620706(2)
Cl–1.5MgO	64.21	21.37	6.38	5.26	0.27	0.13	1.49	0.76	0.09	0.88	0.620706(2)
Cl–2.0MgO	66.22	21.85	5.59	3.08	0.24	0.13	1.99	0.75	0.09	0.56	0.40084(5)
Cl–2.5MgO	65.72	21.44	5.48	3.61	0.23	0.13	2.49	0.75	0.09	0.20	0.40084(5)
Cl–1.5MgO-b	65.34	21.68	6.03	3.75	0.25	0.13	1.49	1.2	0.09	0.79	0.40084(5)
Cl–2.5MgO-b	65.33	21.61	5.42	3.45	0.23	0.13	2.49	1.2	0.09	0.67	0.40084(5)
CC_W	68.74	22.84	4.53	0.57	–	–	0.60	1.03	–	0.36	0.400269(1)
CC_G	65.42	20.99	5.26	3.17	1.10	0.41	1.24	1.15	–	0.71	0.400269(1)

*Loss on ignition at 1000 °C.
Dosages used to obtain the laboratory Portland clinkers, expressed as oxide in weight percent. Elemental composition obtained by XRF of commercial clinkers. Wavelengths used to collect synchrotron X-ray powder diffraction data are also given.

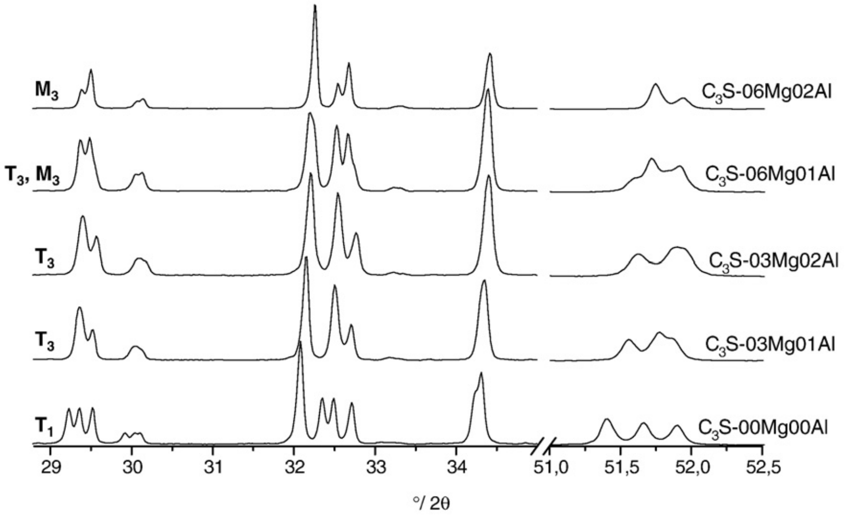

Fig. 1. Selected regions of LXRPD patterns for $Ca_{3-x-y}Mg_xAl_y(Si_{1-y}Al_y)O_5$ nominal series prepared from solid state reaction.

(including anisotropic terms to describe profile broadening if needed), phase fractions and preferred orientation when appropriate.

3. Results and discussion

3.1. Pure C_3S

Five members of the tricalcium silicate solid solutions, Table 1, have been obtained as highly crystalline compounds. The number of thermal treatments up to 1500 °C during 6 h, until no free lime was detected, is given in Table 1. LXRPD patterns for each sample with no free lime were collected and, as an initial characterization, they were inspected in order to identify the stabilized alite form [24]. Fig. 1 shows selected angular ranges of the LXRPD patterns for the prepared samples. In the angular ranges from 31.5 to 33.5° and from 51° to 52.5° (2θ/CuKα), the difference among alites becomes evident. The sample C_3S–00 Mg00Al is triclinic, T_1, as expected, and presents four reflections in the 31.5 to 33.5° angular window, see Fig. 1 bottom. C_3S–03 Mg01Al and C_3S–03 Mg02Al present

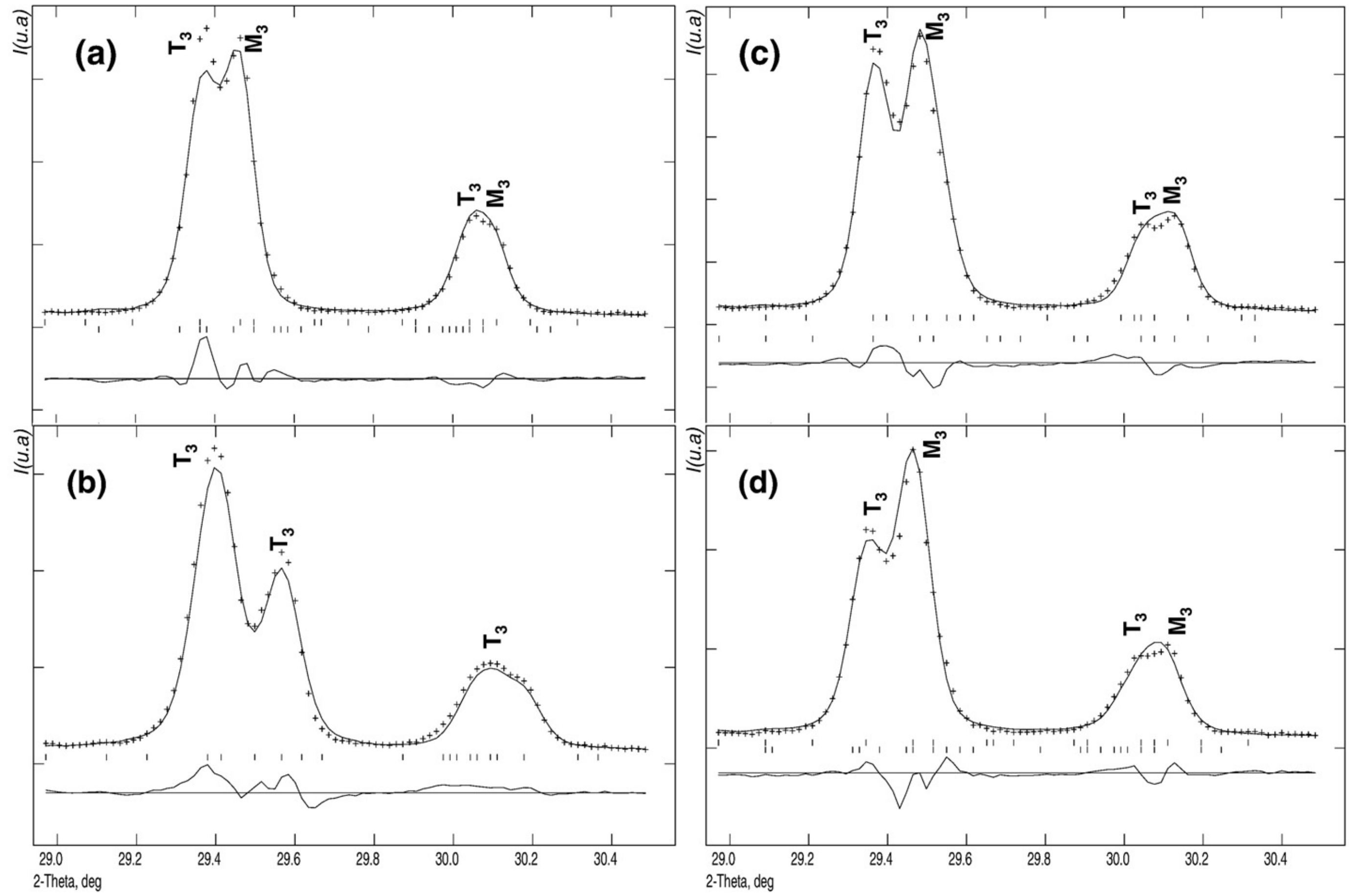

Fig. 2. Selected range [29.0° to 30.5° (2θ)] of the LXRPD Rietveld Plots of (a) C_3S–03 Mg02Al treated once at 1500 °C during 6 h with phase coexistence (T_3 and M_3), (b) C_3S–03 Mg02Al treated twice at 1500 °C during 6 h without phase coexistence (T_3), (c) C_3S–06 Mg01Al treated once at 1500 °C during 6 h with phase coexistence (T_3 and M_3) and (d) C_3S–06 Mg01Al treated twice at 1500 °C during 6 h with phase coexistence (T_3 and M_3).

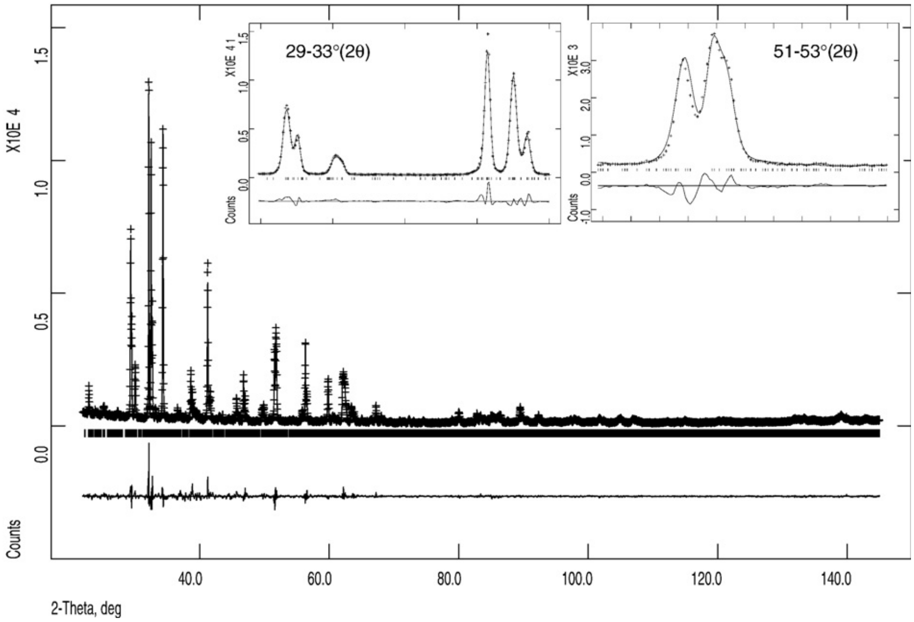

Fig. 3. LXRPD Rietveld plot for nominal $Ca_{2.96}Mg_{0.03}Al_{0.01}(Si_{0.99}Al_{0.01})O_5$ (λ = 1.54 Å). The insets show the fit of two representative regions for alites.

T_3-type powder patterns [11,15], identified by inspecting the angular ranges shown in Fig. 1. Other authors [11,14] studied solid solutions of tricalcium silicate with ZnO and they reported M_1-type powder patterns. These studies [11,14] also stated that T_3 form was not stabilized with ZnO. In the present work, it has not been possible to obtain a M_1-type powder pattern by the addition of magnesium and aluminium in the studied experimental conditions. The nature of the C_3S–06 Mg01Al pattern is discussed just below, and C_3S–06 Mg02Al is clearly M_3 [19,20].

During the ceramic synthesis process another phenomenon was detected. After the first thermal treatment up to 1500 °C during 6 h, C3S–03 Mg02Al and C3 S–06 Mg01Al compositions present phase coexistence [25], i.e., two different crystal structures are needed to fit these patterns. Figs. 2a and c show a selected angular range of the LXRPD Rietveld plots of C3S–03 Mg02Al and C3S–06 Mg01Al, respectively, treated once at 1500 °C during 6 h. A T_3 structural description, obtained in this work (see below), and a M_3 [19] were used to fit these patterns. We decided to perform another thermal treatment to both compositions. Figs. 2b and d show the selected angular range of the LXRPD Rietveld plots of C3S–03 Mg02Al and C3S–06 Mg01Al, respectively, treated twice at 1500 °C. It can be observed that phase coexistence has disappeared for the former composition and only the T_3 structural description was needed to properly fit the pattern. On the other hand, in these experimental conditions C3S–06 Mg01Al still presents phase coexistence (T_3 and M_3 type alites).

3.2. Crystal structure refinement

After the above preliminary study, LXRPD and NPD patterns were collected for the T_3-type sample C_3S–03 Mg01Al, in order to perform a full structural study. As a starting point both structures, T_1 [9] and M_1 [17] were used in the joint refinement using LXRPD and NPD data. However, the published structural description for M_1 is an average

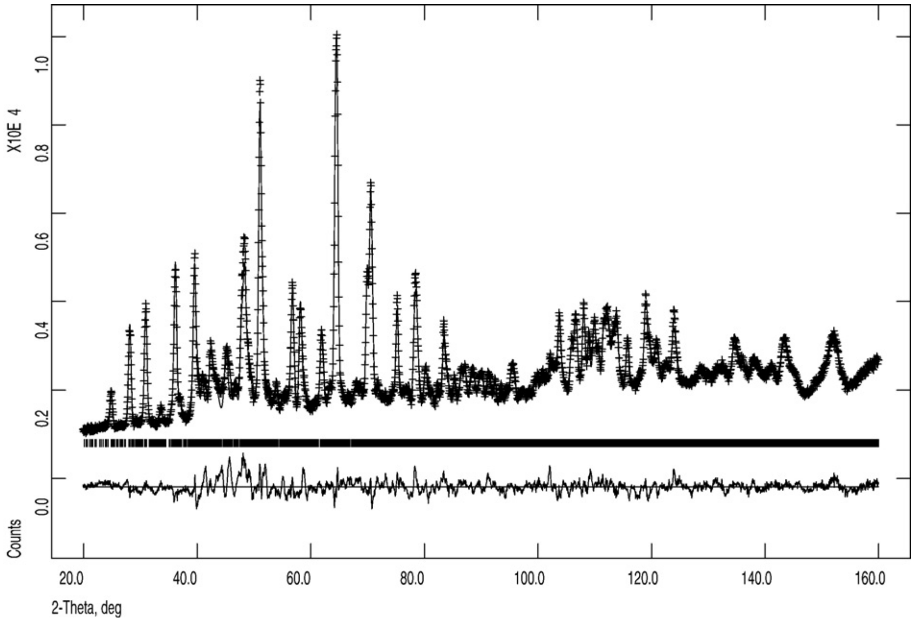

Fig. 4. NPD Rietveld plot for nominal $Ca_{2.96}Mg_{0.03}Al_{0.01}(Si_{0.99}Al_{0.01})O_5$ (λ = 1.1886 Å).

Table 3
Refined atomic parameters for C_3S–03 Mg01Al from a joint refinement using LXRPD, NPD and soft constraints data

Atom	*x*	*y*	*z*
Ca(1)	0.7125(13)	−0.0042(12)	0.9730(9)
Ca(2)	0.3412(12)	0.1623(8)	0.6551(8)
Ca(3)	0.6597(11)	0.3158(12)	0.3223(14)
Ca(4)	0.8223(10)	0.1687(9)	0.1756(11)
Ca(5)	0.1724(12)	0.3346(11)	0.8450(8)
Ca(6)	0.3279(9)	0.4045(10)	0.6432(8)
Ca(7)	0.6707(14)	0.0719(9)	0.3199(10)
Ca(8)	0.0481(9)	0.1693(8)	0.6209(8)
Ca(9)	0.6206(11)	0.1722(10)	0.7089(15)
Ca(10)	0.3768(11)	0.3427(8)	0.3084(8)
Ca(11)	0.9699(10)	0.3405(8)	0.3590(8)
Ca(12)	0.0505(12)	0.3924(12)	0.6259(12)
Ca(13)	0.3402(9)	0.0766(8)	0.2826(10)
Ca(14)	0.6184(11)	0.4245(7)	0.7123(9)
Ca(15)	0.9521(9)	0.0952(9)	0.3673(8)
Ca(16)	0.4761(11)	0.0923(9)	0.8637(93)
Ca(17)	0.2089(12)	0.2377(8)	0.4875(8)
Ca(18)	0.8068(13)	0.2589(10)	0.5240(10)
Ca(19)	0.5490(12)	0.4089(9)	0.1439(9)
Ca(20)	0.6942(10)	0.4931(8)	0.9559(9)
Ca(21)	0.7056(12)	0.2334(10)	0.9653(9)
Ca(22)	0.299211)	0.2688(9)	0.0390(10)
Ca(23)	0.8846(10)	0.0789(9)	0.8098(9)
Ca(24)	0.1381(17)	0.4221(12)	0.1927(11)
Ca(25)	−0.0027(9)	0.2746(8)	0.9969(10)
Ca(26)	0	0	0
Ca(27)	0	0.5	0
Ca(28)	0.5	0.5	0.5
Ca(29)	0.5	0.5	0.5
Si(1)	0.8215(9)	0.4186(7)	0.1603(8)
Si(2)	0.4835(10)	0.3471(8)	0.8684(8)
Si(3)	0.1630(8)	0.0879(8)75	0.8307(7)
Si(4)	0.7998(7)	0.0147(8)	0.5458(7)
Si(5)	0.1919(7)	0.4959(8)	0.4539(8)
Si(6)	0.5183(8)	0.1532(8)	0.1222(8)
Si(7)	0.1412(9)	0.1830(7)	0.2148(8)
Si(8)	0.8683(8)	0.3228(8)	0.7875(7)
Si(9)	0.4805(10)	0.2448(9)	0.5098(8)
O(11)	0.9496(10)	0.4169(8)	0.1222(8)
O(12)	0.7257(10)	0.3838(11)	0.0627(9)
O(13)	0.8175(10)	0.3423(9)	0.2305(9)
O(14)	0.2026(14)	0.4708(8)	0.7742(11)
O(21)	0.4475(14)	0.3950(12)	0.9825(7)
O(22)	0.6226(9)	0.3338(9)	0.8637(11)
O(23)	0.8020(11)	0.2058(9)	0.3540(11)
O(24)	0.4465(10)	0.4181(9)	0.7959(8)
O(31)	0.2862(8)	0.0862(10)	0.7827(9)
O(32)	0.1506(10)	0.1933(8)	0.9102(9)
O(33)	0.1483(9)	0.0024(9)	0.8880(9)
O(34)	0.0639(9)	0.0695(9)	0.7362(8)
O(41)	0.7553(10)	0.0448(9)	0.6592(7)
O(42)	0.6941(4)	−0.0038(9)	0.4580(7)
O(43)	0.8773(9)	0.1021(9)	0.5252(9)
O(44)	0.1226(9)	0.0812(7)	0.4678(9)
O(51)	0.8157(12)	0.4002(8)	0.4611(10)
O(52)	0.3156(5)	0.4952(9)	0.4064(7)
O(53)	0.1864(10)	0.4083(8)	0.5099(9)
O(54)	0.0871(8)	0.4806(9)	0.3639(9)
O(61)	0.5091(14)	0.2641(8)	0.1917(11)
O(62)	0.6421(8)	0.1418(10)	0.0749(8)
O(63)	0.4139(10)	0.1271(12)	0.0320(8)
O(64)	0.5087(12)	0.0795(9)	0.1952(10)
O(71)	0.0135(8)	0.1844(9)	0.2552(9)
O(72)	0.1738(10)	0.0713(7)	0.1622(9)
O(73)	0.2334(10)	0.2244(8)	0.3131(8)
O(74)	0.1430(14)	0.2515(12)	0.1365(11)
O(81)	0.9933(9)	0.3094(10)	0.7437(8)
O(82)	0.8520(11)	0.2478(9)	0.8581(9)
O(83)	0.7646(10)	0.3036(11)	0.6977(8)
O(84)	0.8572(8)	0.4321(8)	0.8632(8)
O(91)	0.5987(13)	0.2302(16)	0.4531(13)
O(92)	0.4058(17)	0.1423(11)	0.4754(13)
O(93)	0.5100(14)	0.2741(10)	0.6336(8)
O(94)	0.4038(16)	0.3312(14)	0.4810(10)
O1	0.2007(9)	0.2864(9)	0.6696(8)
O2	0.4780(11)	0.0432(9)	0.6782(4)
O3	0.6690(30)	0.0788(11)	0.8425(12)
O4	0.0040(12)	0.2518(10)	0.4858(11)
O5	0.3358(27)	0.4181(8)	0.1715(9)
O6	0.1515(7)	0.3915(7)	1.0227(9)
O7	0.8020(11)	0.2058(9)	0.3540(12)
O8	0.8837(11)	0.1395(7)	1.0092(13)
O9	0.5521(12)	0.4574(9)	0.3288(6)

The thermal factors are given in the text.

structure, so many experimental peaks were not indexed which led to a poor fit. The triclinic T_1-form was a much better starting point. The triclinic structural description has 83 crystallographically independent sites: 29 Ca [4 in special position (*x*0*z*) and 25 in general position]; 9 Si all in general position; and 45 O all in general position. The joint Rietveld refinement with LXRPD and NPD patterns gave some chemically unrealistic interatomic distances. Thus, a third histogram containing soft constraints was included to have a chemically correct structural model. We have soft constrained [26] all SiO_4 tetrahedra by imposing 36 Si–O bond distances of 1.63(3) Å and 54 O···O intra-tetrahedral distances of 2.66(6) Å. It was also necessary to include 128 Ca–O soft constraints of 2.40(4) Å for all Ca–O distances that converged to values shorter than 2.30 Å. The final weighting factor for the soft constraint histogram was 200.

241 atomic parameters were refined in the final cycle. This structure is triclinic and fits properly a T_3-type powder diffraction pattern. It has a P $\bar{1}$ space group with $a=11.6389(2)$ Å, $b=14.1716(3)$ Å, $c=13.6434(3)$ Å, $\alpha=104.982(2)^\circ$, $\beta=94.622(1)^\circ$, $\gamma=90.107(2)^\circ$ and $V/Z=120.346(6)$ Å^3. In the final model, we refined four different isotropic displacement parameters, U_{iso}: one for the Ca-atoms, 0.0071(5) Å^2; a second for the silicons, 0.008(1) Å^2; a third for the oxygens belonging to the SiO_4 tetrahedra, 0.0119(1) Å^2 and a final one for the oxides anions, 0.035(2) Å^2. The final *R*-factors were $R_{WP}=10.8\%$ and $R_F=4.7\%$ for the LXRPD data and $R_{WP}=5.5\%$ and $R_F=4.3\%$ for the NPD data. The Rietveld plots for the LXRPD and NPD data are given in Figs. 3 and 4, respectively. Table 3 shows final atomic parameters.

Pure C_3S powder patterns were revised using (when appropriate) the T_3 structure description presented above. In Table 4, the refined unit cell parameters obtained in the Rietveld analyses are given. In this table unit cell values of C_3S–03 Mg01Al are also included, for the sake of comparison. Stoichiometric C_3S was fit with the T_1 structural description of Golovastikov et al. [9]. The sample with phase coexistence (C_3S–06 Mg01Al) was fitted with T_3 and M_3 alites. Finally, we concluded that the samples with $x=0.03$, [0.53 wt.% expressed as MgO] C_3S–03 Mg01Al and C_3S–03 Mg02Al, are T_3-type and their powder patterns are better fitted with the T_3 structural description presented in this work. On the other hand, we have observed that the increase in the aluminium content decrease the volume of the C_3S stabilized [27], as expected.

3.3. Rietveld quantitative phase analyses of clinkers

Laboratory Portland clinkers were prepared with different amounts of magnesium, Table 2, in order to cause polymorphic changes in C_3S. In a first visual inspection of SXRPD patterns, Fig. 5, it is noticeable that C_3S peak positions are shifted to lower d-spacings (larger 2-theta values). This behavior was expected as Mg^{2+} radius is smaller than that of Ca^{2+}. On the other hand, it was proved that low contents of magnesium have promoted T_3-type C_3S stabilization and that M_3 alite presence was important as the amount of MgO increases, as expected [12]. So, in clinker with 0.4 wt.% of MgO, Cl–0.4MgO, the T_3 structural description, proposed in this work, was the best one to fit the main phase. It has to be highlighted that other authors [12,17] state that alites (pure or in

Table 4
Rietveld refined unit cell parameters and volume of pure members of tricalcium silicate solid solution

Sample (polymorph)	*a*/Å	*b*/Å	*c*/Å	*α* /°	*β* /°	*γ* /°	*V*/*Z*/Å^3
C_3S–00 Mg00Al (T_1)	11.6385(2)	14.2152(2)	13.6913(2)	105.293(1)	94.567(1)	89.846(1)	120.978(4)
C_3S–03 Mg01Al (T_3)	11.6389(3)	14.1716(3)	13.6434(3)	104.982(2)	94.622(1)	90.107(2)	120.346(6)
C_3S–03 Mg02Al (T_3)	11.6167(2)	14.1581(3)	13.6268(3)	105.005(2)	94.612(1)	90.108(1)	119.843(5)
C_3S–06 Mg01Al (T_3, M_3)	11.6619(7)	14.1675(6)	13.6431(8)	104.981(5)	94.774(3)	90.098(4)	120.518(9)
	33.1442(8)	7.0427(1)	18.5380(4)	90.00(−)	94.198(2)	90.00(−)	119.879(5)
C_3S–06 Mg02Al (M_3)	33.1056(2)	7.04005(9)	18.5335(2)	90.00(−)	94.167(1)	90.00(−)	119.670(4)

clinkers) with low amount of magnesium content presents M_1-like powder pattern. However, we show that these alites can be properly fitted with a triclinic form, which corresponds to a T_3 [15,16]. On the other hand, clinkers with the highest amounts of magnesium oxide, Cl–2.5MgO and Cl–2.5MgO–b contained M_3–C_3S form [19]. The remaining clinkers presented C_3S phase coexistence [25], and therefore, two structural descriptions were used. T_3-type C_3S structure was used to describe the alite with larger volume and a M_3-type C_3S structure to fit that with smaller volume. Fig. 6 shows ranges of the Rietveld plots of Cl–0.4MgO, Cl–1.5MgO and Cl–2.5MgO, where the main peaks due to a given phase have been labeled. Phase coexistence is clearly evident when high resolution data, i.e. SXRPD or strictly monochromatic LXRPD data are used. High-resolution data allow obtaining more accurate quantitative phase analyses.

Table 5 gives Rietveld quantitative phase analysis results of laboratory Portland clinkers obtained from SXRPD data. In this table, the theoretical mineralogical compositions, derived by Bogue calculations [28], are also given in italics. From results in Table 5, it is noteworthy that minor elements, such as magnesium or sulfur, affect the mineralogical composition, and Bogue calculations ignore these phenomena. As magnesium content increases more C_3S is formed, and some authors concluded that hydraulic properties are also enhanced [29].

Fig. 7 shows the evolution of the refined volume (*V*/*Z*) of alites in laboratory Portland clinkers as a function of magnesium content. In this figure clinkers with different amount of SO_3 have been identified with different symbols, open squares stands for clinkers with 0.75 wt.% of SO_3 and solid circles for clinkers with 1.20 wt.% of SO_3. It can be observed that volume decreases as magnesium content increases, as expected. On the other hand, for a fixed MgO content, the C_3S volume is larger when SO_3 wt.% increases. The alite refined volume value in clinkers obtained by Rietveld analysis can be a useful tool to predict the amount of MgO in the clinker, in the case of the lack of chemical information. It could be affirmed that a clinker containing an alite with a refined volume value between 121.0 and 120.3 Å^3 should contain up to ~1.0 wt.% of MgO and a clinker with a C_3S V/Z

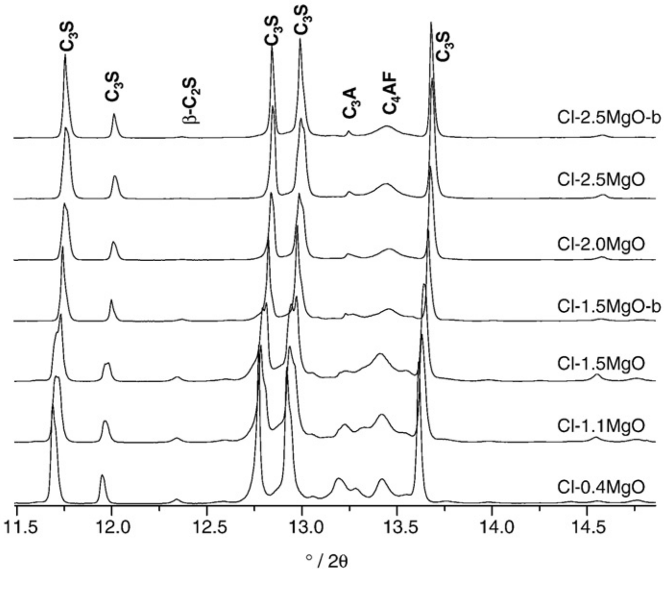

Fig. 5. SXRPD patterns for laboratory clinkers with different amounts of magnesium oxide. Main peaks due a given phase have been labeled.

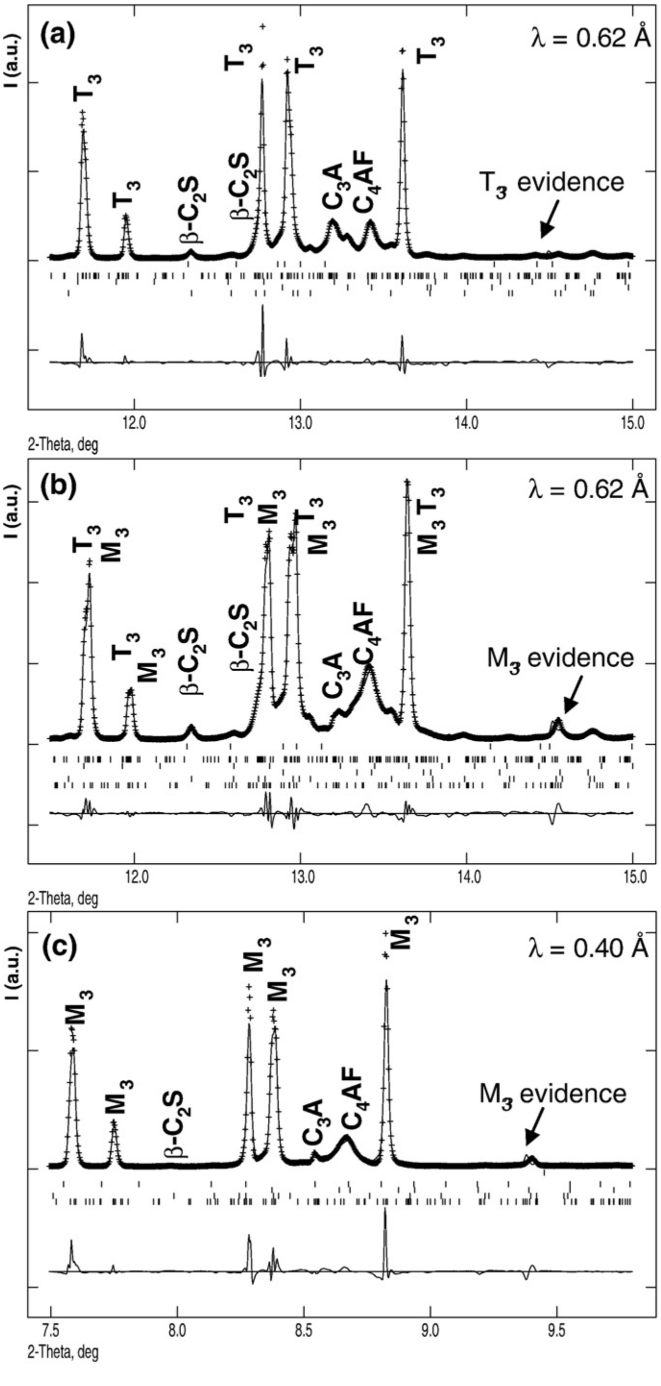

Fig. 6. SXRPD Rietveld plots for (a) Cl–0.4MgO, (b) Cl–1.5MgO and (c) Cl–2.5MgO. Main peaks due to a given phase have been labelled.

Table 5
Phase composition (weight percentage) for laboratory Portland clinkers from Rietveld refinements using SXRPD data

	C_3S (T_3)	C_3S (M_3)	C_3S _ total	β-C_2S	α'$_H$-C_2S	C_2S _ total	C_4AF	C_3A	Rwp/%
Cl–0.4MgO	60.2(1)	–	60.2	13.3(2)	2.6(1)	15.9	14.0(1)	9.9(2)	13.0
			56.5			*18.1*	*15.8*	*7.9*	
Cl–1.1MgO	24.0(3)	33.5(3)	57.5	16.0(2)	3.7(2)	19.7	17.4(1)	5.4(1)	9.1
			51.2			*22.5*	*15.9*	*8.0*	
Cl–1.5MgO	18.1(3)	38.0(3)	56.1	18.8(2)	2.6(2)	21.4	19.6(1)	2.9(1)	8.8
			48.6			*24.7*	*16.0*	*8.0*	
Cl–2.0MgO	29.1(4)	48.4(3)	77.5	4.5(2)	1.6(1)	6.1	12.7(2)	3.7(2)	11.5
			61.5			*16.2*	*9.4*	*9.6*	
Cl–2.5MgO$^\#$	–	81.8(1)	81.8	1.0(2)	–	1.0	15.5(1)	1.4(1)	8.7
			62.5			*14.3*	*11.0*	*8.4*	–
Cl–1.5MgO-b	29.7(3)	35.5(3)	65.2	12.5(2)	2.6(1)	15.1	14.2(1)	5.5(1)	10.9
			55.3			*20.4*	*11.4*	*9.6*	
Cl–2.5MgO-b	–	78.0(1)	78.0	2.7(2)	3.3(2)	6.0	13.9(2)	2.1(3)	15.1
			60.3			*16.5*	*10.5*	*8.5*	–

$^\#$Also contains 0.30(5) wt.% of MgO.
Mineralogical compositions derived from Bogue calculations are given in italics. Agreement factors of the fits are also given.

Table 6
Phase composition (weight percentage) for commercial Portland clinkers from Rietveld refinements using SXRPD and LXRPD data

		C_3S (T_1)	C_3S (T_3)	C_3S (M_3)	C_3S _ total	β-C_2S	C_4AF	C_3A	Rwp/%
CC_W SXRPD	T_1:	67.3(1)	–	–	67.3	29.3(2)	–	3.4(1)	16.7
	T_3:	–	69.5(1)	–	69.5	27.1(2)	–	3.4(1)	13.4
	M_3:	–	–	70.0(1)	70.0	26.7(2)	–	3.3(19)	13.9
CC_W LXRPD	T_1:	70.6(2)	–	–	70.6	25.2(5)	–	4.2(2)	10.2
	T_3:	–	74.7(2)	–	74.7	21.6(4)	–	3.7(2)	8.2
	M_3:	–	–	75.3(2)	75.3	21.4(3)	–	3.3(1)	10.9
CC_W Bogue					73.2	10.3	1.7	11.0	
CC_G$^\$$ SXRPD	T_1:	62.6(2)	–	–	62.6	12.6(2)	13.0(1)	7.9(1)	17.4
	T_3:	–	64.4(2)		64.4	10.5(2)	13.1(1)	9.0(1)	15.0
	M_3:	–	–	66.0(2)	66.0	9.6(2)	12.6(1)	9.3(1)	16.4
	T_3+M_3:	–	29.4(1)	36.3(1)	65.7	10.8(2)	12.1(1)	8.7(1)	8.9
CC_G$^\$$ LXRPD	T_1:	65.9(3)	–	–	65.9	9.0(6)	12.9(3)	9.6(2)	6.9
	T_3:	–	66.0(4)	–	66.0	8.8(5)	13.1(3)	9.4(2)	6.5
	M_3:	–		66.6(3)	66.6	11.1(6)	12.3(3)	8.7(2)	7.5
	T_3+M_3:	–	32.2(4)	33.5(4)	65.7	10.3(4)	12.2(2)	9.2(2)	5.1
CC_G Bogue					*58.8*	*15.9*	*9.6*	*8.6*	

$^\$$Also contains 2.0(1) wt.% of $NaK_3(SO_4)_2$ and 0.7(1) wt.% of MgO.
T_1, T_3 and M_3 structural description have been tested. Mineralogical composition derived with Bogue calculations (in italics) and agreement factors of the fits are also given.

refined smaller than ~119.8 Å^3 may contain more than 2.1 wt.% of MgO. In the studied experimental conditions, clinkers with magnesium content between 1.0 and 2.1 wt.% have displayed phase coexistence, but this range cannot be directly extrapolated to commercial materials as it will depend on the presence of (other) foreign ions in alites.

Finally, the T_3 structural description obtained in this work was also used to analyze commercial Portland clinkers with low magnesium content. Two commercial clinkers (MgO-contents given in Table 2) were chosen, one white Portland clinker, CC_W, and one grey Portland clinker, CC_G. Table 6 gives quantitative phase analyses of these two clinkers using T_1, T_3 and M_3 structural descriptions. It is clearly seen that the use of the T_3 structural description resulted in better fits, i.e. lower R_{WP} values, Table 6. Fig. 8(a) shows a selected range of the SXRPD pattern of CC_W, where main peaks have been labeled, with alite displaying a T_3-type pattern. On the other hand, CC_G clinker presented phase coexistence, so the use of a single structural description yielded non-satisfactory fits, Table 6. Finally, T_3 and M_3 structural descriptions were used obtaining the best refinement results. Fig. 8(b) shows the same range of the SXRPD pattern as in the white clinker, where main alite peaks are clearly split due to the phase coexistence. Although, T_3 description yields better fits, quantitative phase analyses results are not strongly affected by the choice of the structural description. Thus, small changes in cement manufacture process, for example, a slightly different chemical composition of raw materials, are not a severe problem if the Rietveld method is being used in on-line quality control.

Fig. 9 shows selected angular ranges of the Rietveld plots for both commercial clinkers collected with different wavelengths, i. e. Fig. 9a and c are SXRPD patterns (λ=0.40 Å) of these commercial clinkers,

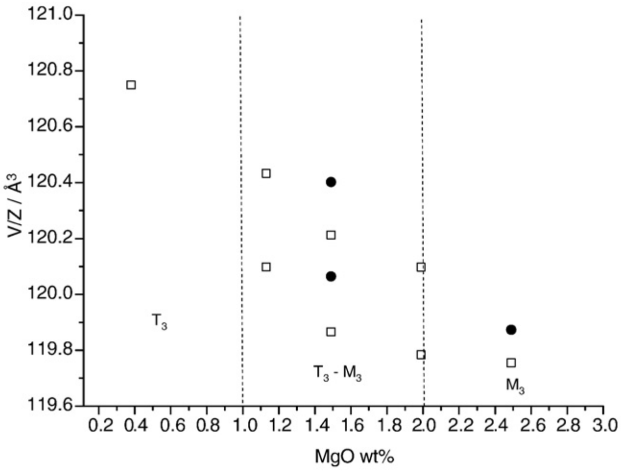

Fig. 7. Refined volume (V/Z) of C_3S of laboratory Portland clinkers as a function of the overall MgO weight percentage. Open squares stand for clinkers with 0.75 wt.% of SO_3 and solid circles stand for clinkers with 1.20 wt.% of SO_3.

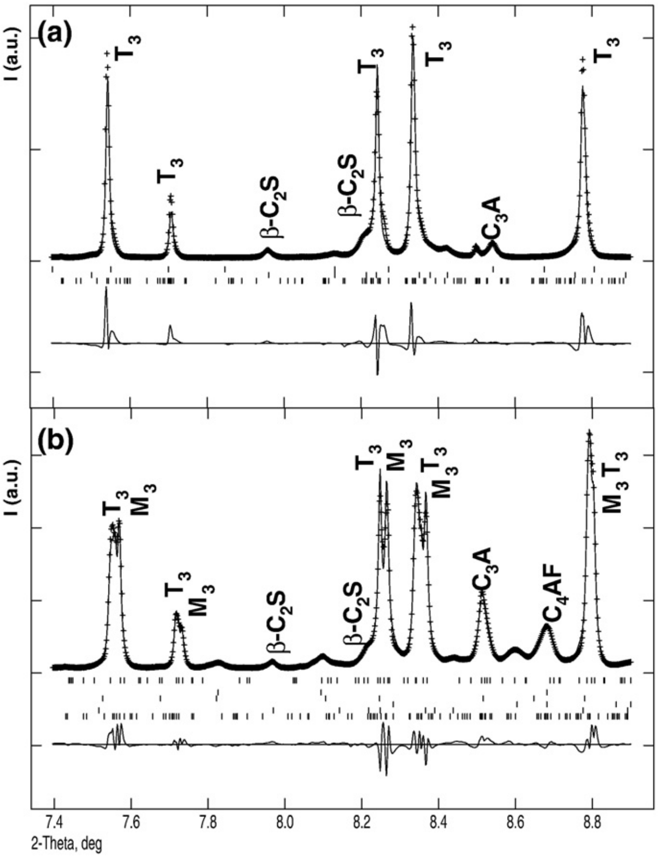

Fig. 8. SXRPD Rietveld plots for (a) CC_W (white Portland clinker) and (b) CC_G (grey Portland clinker). Main peaks due to a given phase have been labelled.

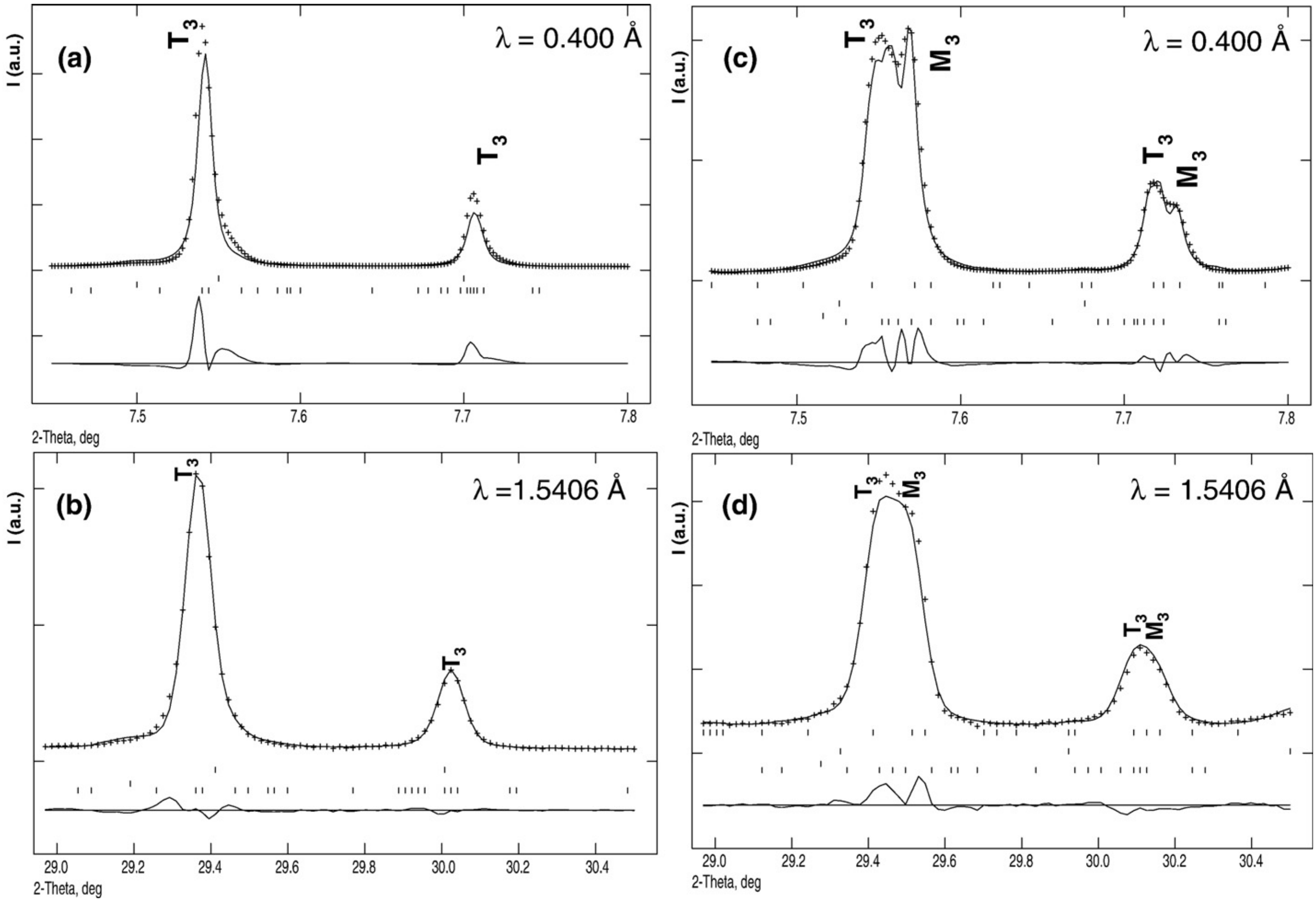

Fig. 9. Selected range [7.45° to 7.80° (2*θ*)] of the SXRPD Rietveld Plots of (a) CC_W (white Portland clinker) and (c) CC_G (grey Portland clinker). Selected range [29° to 30.5° (2*θ*)] of the LXRPD Rietveld Plots of (b) CC_W (white Portland clinker) and (d) CC_G (grey Portland clinker).

meanwhile Fig. 9b and d show patterns collected for the same samples but with monochromatic LXRPD ($\lambda = 1.54$ Å). Fig. 9 highlights the convenience of using two appropriate structural descriptions to fit alites in commercial clinkers with intermediate magnesium contents, especially when using high resolution data. Rietveld quantitative phase analysis results using LXRPD data are also shown in Table 6. These analyses corroborate the conclusions drawn from the SXRPD study: T_3 structural description for alites, in low magnesium content clinkers, yields the best fits.

4. Conclusions

A new structural description for low magnesium-bearing alite has been derived by combined XRPD, NPD and soft-constrained Rietveld refinement. The reported T_3-type alite structure fits patterns of alites in laboratory and commercial clinkers which are described as T_3- and/or M_1-type(s). This new T_3 structure fits properly alites in clinkers with $MgO < 1.0$ wt.%. The use of two structural descriptions for alite, i.e. T_3 and M_3, in Rietveld quantitative phase analysis is advisable when high resolution data are recorded for clinkers with intermediate MgO content. Finally, we highlight that three room-temperature crystal structures are already available for alite: T_1 for stoichiometric C_3S, T_3 for low magnesium content alites and M_3 for high-Mg content alites.

Acknowledgments

We thank financial support from P06-FQM-01348 research project (Junta de Andalucía, Spain). ESRF is thanked for the provision of X-ray synchrotron powder diffraction beamtime. This work was partially performed at the spallation neutron source SINQ, Paul Scherrer Institut, Villigen, Switzerland.

References

[1] I.C. Madsen, N.V.Y. Scarlett, L.M.D. Cranswick, T. Lwin, Outcomes of the International Union of Crystallography Commission on powder diffraction round robin on quantitative phase analysis: samples 1a to 1 h, J. Appl. Crystallogr. 34 (2001) 409–426.
[2] N.V.Y. Scarlett, I.C. Madsen, L.M.D. Cranswick, T. Lwin, E. Groleau, G. Stephenson, M. Aylmore, N. Agron-Olshina, Outcomes of the International Union of Crystallography Commission on powder diffraction round robin on quantitative phase analysis: samples 2, 3, 4, synthetic bauxite, natural granodiorite and pharmaceuticals, J. Appl. Crystallogr. 35 (2002) 383–400.
[3] A.G. De la Torre, A. Cabeza, A. Calvente, S. Bruque, M.A.G. Aranda, Full phase analysis of Portland clinker by penetrating synchrotron powder diffraction, Anal. Chem. 73 (2001) 151–156.
[4] N.V.Y. Scarlett, I.C. Madsen, C. Manias, D. Retallack, On-line X-ray diffraction for quantitative phase analysis: application in the Portland cement industry, Powder Diffr. 16 (2001) 71–80.
[5] A.G. De la Torre, M.A.G. Aranda, Accuracy in Rietveld quantitative phase analysis of Portland cements, J. Appl. Crystallogr. 36 (2003) 1169–1176.
[6] V.K. Peterson, A.S. Ray, B.A. Hunter, A comparative study of Rietveld phase analysis of cement clinker using neutron, laboratory X-ray, and synchrotron data, Powder Diffr. 21 (1) (2006) 12–18.
[7] L.D. Mitchell, J.C. Margeson, P.S. Whitfield, Quantitative Rietveld analysis of hydrated cementitious systems, Powder Diffr. 21 (2) (2006) 111–113.
[8] M. Merlini, G. Artioli, C. Meneghini, T. Cerulli, A. Bravo, F. Cella, The early hydration and the set of Portland cements: in situ X-ray powder diffraction studies, Powder diffr. 22 (3) (2007) 201–208.
[9] N.I. Golovastikov, R.G. Matveeva, N.V. Belov, Crystal structure of the tricalcium silicate $3CaO \cdot SiO_2 = C_3S$, Sov Phys Crystallogr 20 (4) (1975) 441–445.
[10] H.F.W. Taylor, Cement Chemistry, Academic Press, London, 1997.
[11] M. Bigare, A. Guinier, C. Mazieres, M. Regourd, N. Yannaquis, W. Eysel, T.H. Hahn, E. Woermann, Polymorphism of tricalcium silicate and its solid solutions, J. Am. Ceram. Soc. 50 (11) (1967) 609–619.

[12] I. Maki, K. Goto, Factors influencing the phase constitution of alite in Portland cement clinker, Cem. Concr. Res. 12 (3) (1982) 301–308.

[13] F. Dunstetter, M.N. de Noirfontaine, M. Courtial, Polymorphism of tricalcium silicate, the major compound of Portland cement clinker 1. Structural data: review and unified analysis, Cem. Concr. Res. 36 (2006) 39–53.

[14] K. Urabe, H. Nakano, H. Morita, Structural modulation in monoclinic tricalcium silicate solid solutions doped with zinc oxide, M(I), M(II), and M(III), J. Am. Ceram. Soc. 85 (2) (2002) 423–429.

[15] V.K. Peterson, A Rietveld refinement investigation of a Mg-stabilized triclinic tricalcium silicate using synchrotron X-ray powder diffraction data, Powder Diffr. 19 (4) (2004) 356–358.

[16] V.K. Peterson, Powder diffraction investigations of cement and its major component, tricalcium silicate. PhD thesis, (2003), http://adt.lib.uts.edu.au/public/adtNTSM20040830.173127/index.html.

[17] M.N. De Noirfontaine, F. Dunstetter, M. Courtial, G. Gasecki, M. Signes-Frehel, Polymorphism of tricalcium silicate, the major compound of Portland cement clinker 2. Modelling alite for Rietveld analysis, an industrial challenge, Cem. Concr. Res. 36 (2006) 54–64.

[18] F. Nishi, Y. Takeuchi, The rhombohedral structure of tricalcium silicate at 1200 °C, Z. Kristallogr. 168 (1984) 197–212.

[19] A.G. De la Torre, S. Bruque, J. Campo, M.A.G. Aranda, The superstructure of C_3S from synchrotron and neutron powder diffraction and its role in quantitative phase analyses, Cem. Concr. Res. 32 (2002) 1347–1356.

[20] F. Nishi, Y. Takeuchi, I. Maki, Tricalcium silicate $Ca_3O[SiO_4]$: the monoclinic superstructure, Z. Kristallogr. 172 (1985) 297–314.

[21] P. Fischer, G. Frey, M. Koch, M. Könnecke, V. Pomjakushin, J. Schefer, R. Thut, N. Schlumpf, R. Bürge, U. Greuter, S. Bondt, E. Berruyer, High-resolution powder diffractometer HRPT for thermal neutrons at SINQ, Phys. B, 276 (2000) 146–147.

[22] H.M. Rietveld, A profile refinement method for nuclear and magnetic structures, J. Appl. Crystallogr. 2 (1969) 65–71.

[23] A.C. Larson, R.B. Von Dreele, General Structure Analysis System (GSAS), Los Alamos National Laboratoy Report LAUR-86-748, 1994, GSAS @ program http://public.lanl.gov:80/gsas/.

[24] M. Courtial, M.N. de Noirfontaine, F. Dunstetter, G. Gasecki, M. Signes-Frehel, Polymorphism of tricalcium silicate in Portland cement: a fast visual identification of structure and superstructure, Powder diffr. 18 (2003) 7–15.

[25] A.G. De la Torre, E.R. Losilla, A. Cabeza, M.A.G. Aranda, High-resolution synchrotron powder diffraction analysis of ordinary portland cements: phase coexistence of alite, Nucl. Instrum. Methods B238 (2005) 87–91.

[26] R.A. Young, The Rietveld method, Oxford University Press, Oxford, 1993.

[27] J.M. Porras-Vázquez, A.G. Dela Torre, E.R. Losilla, M.A.G. Aranda, Oxide and proton conductivity in aluminum-doped tricalcium oxy-silicate, Solid State Ionics 178 (15–18) (2007) 1073–1080.

[28] R.H. Bogue, Calculation of the compounds in Portland cement, Ind. Eng. Chem. Analytical Edition. 1 (4) (1929) 192–197.

[29] N.K. Katyal, S.C. Ahluwalia, R. Parkash, Solid solution and hydration behaviour of magnesium-bearing tricalcium silicate phase, Cem. Concr. Res. 28 (6) (1998) 867–875.